Ultrafast carriers dynamics in filled-skutterudites

Liang Guo,[1] Xianfan Xu,[1,a)] and James R. Salvador[2]
[1]School of Mechanical Engineering and Birck Nanotechnology Center, Purdue University, West Lafayette, Indiana 47907, USA
[2]Chemical and Materials Systems Laboratory, GM Global R&D, Warren, Michigan 48090, USA

(Received 28 April 2015; accepted 1 June 2015; published online 9 June 2015)

Carrier dynamics of filled-skutterudites, an important class of thermoelectric materials, is investigated using ultrafast optical spectroscopy. By tuning the wavelength of the probe laser, charge transfers at different electronic energy levels are interrogated. Analysis based on the Kramers-Kronig relation explains the complex spectroscopy data, which is mainly due to band filling caused by photo-excited carriers and free carrier absorption. The relaxation time of hot carriers is found to be about 0.4–0.6 ps, depending on the electronic energy level, and the characteristic time for carrier-phonon equilibrium is about 0.95 ps. These studies of carrier dynamics, which fundamentally determines the transport properties of thermoelectric material, can provide guidance for the design of materials. © *2015 AIP Publishing LLC*. [http://dx.doi.org/10.1063/1.4922399]

Binary skutterudites have the general chemical formula MX_3, where M denotes a transition metal atom and X represents a pnictogen atom. The unit cell is made of eight cubes framed by the M atoms, six of which are filled by mutually orthogonal X_4 rings, forming icosahedral cages located at the corner and center of the unit cell. It has been proposed[1] and verified that filling the residual cages with proper guest atoms can considerably decrease the lattice thermal conductivity.[2–5] Thus, filled-skutterudites have stimulated much interest as a thermoelectric material due to their high figure of merit (ZT) at high temperature.[6–10]

Previous studies have been focused on the mechanism of lattice thermal conduction suppression by filling with foreign atoms and improving the ZT value. For example, studies using Raman spectroscopy,[11] heat capacity measurement together with inelastic neutron scattering,[12,13] and infrared reflectance spectroscopy[14] claim that the filled atoms behave as local rattlers to scatter phonons resulting in lower thermal conductivity. On the other hand, a study by neutron spectroscopy and *ab initio* calculation finds well defined phase relations between the guest and the host atom dynamics,[15] contrary to the conception of rattler atoms. Other mechanisms are also proposed including anharmonic interaction between the host and the guest atoms[16] and distortion of the host lattice.[17]

While the lattice thermal conductivity is an important concern, transport properties of carriers (electrons or holes) also fundamentally determine the quality of a thermoelectric material through affecting both thermal and electrical transport processes, which have been rarely explored for filled-skutterudites. In this work, we investigate the carrier dynamics of filled-skutterudites in the time domain using ultrafast spectroscopy, which was previously applied to examining the interactions between the host lattice and the guest atoms[18,19] and acoustical phonon dynamics in filled-skutterudites.[20] By varying the probe wavelength, different electronic energy levels are interrogated, which allows for analysis of the physical processes and the extraction of the transport properties of the carriers. The method and the analysis of this work can be extended to obtain more detailed information about the carrier dynamics such as individual relaxation times of electrons and holes. Such information is important for understanding and optimizing skutterudite-based thermoelectric materials.

Ultrafast spectroscopy used in this work is based on a reflection geometry. The femtosecond laser pulses are generated from a Ti:sapphire amplified laser system with a central wavelength of 800 nm and a repetition rate of 5 kHz. A beamsplitter divides the output laser into two beams. One is used as a pump for exciting the carriers and the other as a probe, the wavelength of which is tuned by an optical parametric amplifier (OPA) with tuning range from 490 to 1600 nm. The pulse width (full width at half maximum) of the pump laser is about 70 fs. The pump laser is modulated by a mechanical chopper at 500 Hz and the transient reflectance signal is collected by a lock-in amplifier with the reference frequency set at 500 Hz to increase the signal-to-noise ratio.

The skutterudite sample is made through melting Co and Sb in an atom number ratio of 1:3 by induction followed by adding the filling species, misch-metal and Fe, to the desired composition. The ingot after solidification is annealed for two weeks to get the target composition. The composition of the sample for measurement is $Mm_{0.65}Fe_{2.92}Co_{1.08}Sb_{11.98}$, where Mm represents misch-metal, a mixture of rare-earth elements including mainly Ce, La, Nd, and Pr. Co is partially substituted by Fe to keep charge balance. The sample is *p*-type with hole concentration $5.6 \times 10^{20}\,cm^{-3}$. The doped impurity concentration may be high enough to overlap the ground state wavefunction of holes on nearby impurity atoms significantly, and thus produce impurity bands. However, based on the previous *ab initio* calculation results for filled CoP_3-based skutterudites,[21] the dominant influence is the shift of the Fermi level, whereas the band structure is affected only to a small extent even when the doping ratio is as high as that of $La_{0.5}Co_4P_{12}$.

The transient reflectance signals with varied probe wavelengths are shown in Fig. 1 within a measurement time

a)Author to whom correspondence should be addressed. Electronic mail: xxu@purdue.edu

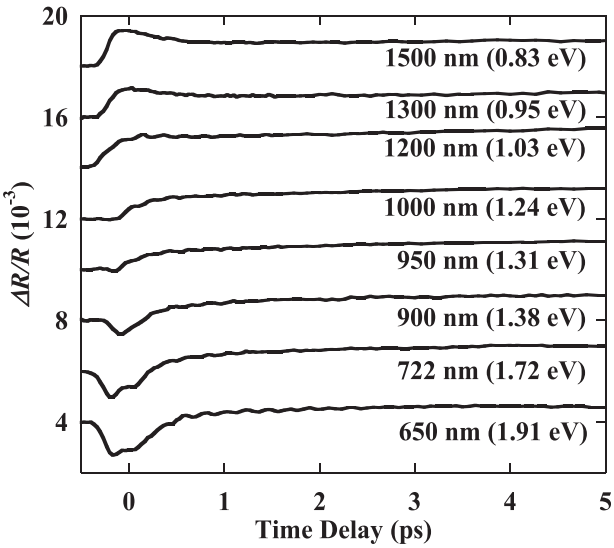

FIG. 1. The transient reflectance signals of $Mm_{0.65}Fe_{2.92}Co_{1.08}Sb_{11.98}$ with pump wavelength 800 nm and probe wavelength from 1500 to 650 nm. The pump fluence is 0.42 mJ/cm^2. The zero time delay is not exact since the light path length changes slightly when the probe wavelength is varied due to the wavelength-dependent index of refraction and the change of the optics in OPA when the probe wavelength is varied.

(probe delay) of 5 ps, which clearly shows the dependence of the signal on the probe wavelength. The curves are shifted vertically for clarity. The pump fluence is 0.42 mJ/cm^2. For estimation, the reflectance at 800 nm is taken as 0.6 (Ref. 22) and the absorption coefficient $5 \times 10^5\,\mathrm{cm}^{-1}$,[23] which render a photoexcited carrier density of $3.4 \times 10^{19}\,\mathrm{cm}^{-3}$. When the probe wavelength is longer than 1000 nm, the signal shows a fast increase followed by a fast decay within the first 1 ps. As the probe wavelength decreases, the fast increasing and decaying is reversed to a fast decrease followed by a fast recovery, also within the first 1 ps. A slower rise of a few ps following the fast component is observed for all the probe wavelengths, which is attributed to free carrier absorption.

The fast-varying increase or decrease is attributed to band filling caused by photoexcitation and relaxation of the carriers. According to the *ab initio* calculation for $CoSb_3$- and hypothetical $FeSb_3$-based skutterudites,[23–27] the band edge states that determine the band gap contribute little to the density of states (DOS), while the states farther away from the band edge contribute much more. This results in a pseudogap, which for $CoSb_3$- and $FeSb_3$-based skutterudites is predicted to be less than 0.7 eV (1771 nm), and has been verified by measurements of temperature-dependent electrical resistivity.[7] The laser pulses used in this work (800 nm pump and 650–1500 nm probe) all have energy greater than the pseudogap, therefore the laser pulses induce interband transition. The optical response can then be attributed to band filling, band gap renormalization, and free carrier absorption.[28,29] Band gap renormalization is due to considerable overlapping of the wavefunction of the carriers with large density. In this work, the photoexcited carrier density is on the order of $10^{19}\,\mathrm{cm}^{-3}$ which is calculated under the approximation that all the excitation energy is absorbed through interband transition, and is much lower than the doped carrier concentration $5.6 \times 10^{20}\,\mathrm{cm}^{-3}$. Moreover, some of the laser energy is absorbed by the doped free carriers through intraband transition, thus the change of the carrier density is even smaller. Therefore, the band gap renormalization has negligible contribution, and the signal is attributable to band filling and free carrier absorption.

The reason for the increase vs. decrease of the initial optical signal based on the probe wavelength is explained in terms of the change in the dielectric constant $\varepsilon = \varepsilon_1 + i\varepsilon_2$. As illustrated in Fig. 2(a), the pump excites electrons from the valence band into the conduction band, leaving the same number of holes in the valence band. Distributions of photoexcited electrons and holes at high energy levels immediately after the excitation are determined by the pump photon energy E_{pump}. Accordingly, the absorption decreases at the pump wavelength λ_{pump} (800 nm in this work) due to band filling by the excited electrons and holes, and the imaginary part ε_2 of the dielectric constant as this wavelength decreases. The change of the real part $\Delta\varepsilon_1$ is related to $\Delta\varepsilon_2$ through the Kramers-Kronig relation[30]

$$\Delta\varepsilon_1(\omega_0) = \frac{2}{\pi} P \int_0^\infty \frac{\omega \Delta\varepsilon_2(\omega)}{\omega^2 - \omega_0^2} d\omega, \tag{1}$$

where P denotes the Cauchy principal value. The decrease in ε_2 produces a "sink," as shown in Fig. 2(b) (the upper red curve). On the shorter wavelength side of the ε_2 sink, $\Delta\varepsilon_2 < 0$ and $\omega^2 - \omega_0^2 < 0$, resulting in $\Delta\varepsilon_1 > 0$ according to Eq. (1); while on the longer wavelength side of the ε_2 sink, the resulting $\Delta\varepsilon_1 < 0$. These qualitative wavelength dependences of $\Delta\varepsilon_1$ and $\Delta\varepsilon_2$ are illustrated in the upper part of Fig. 2(b). As

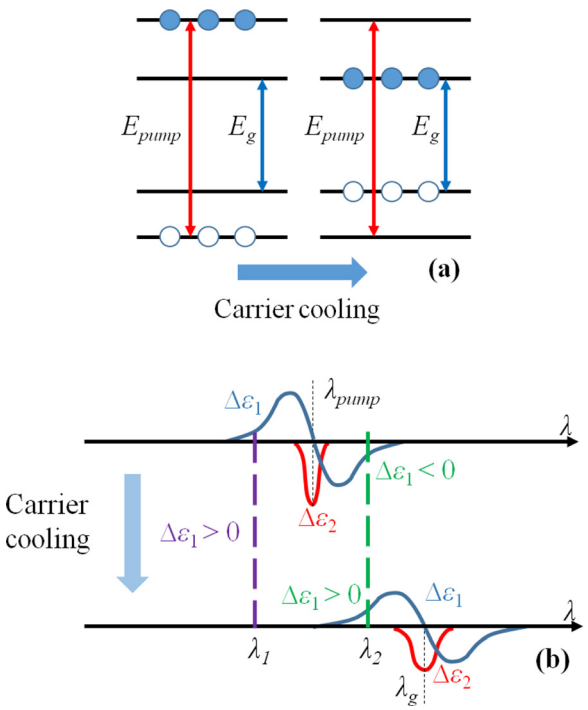

FIG. 2. Evolution of the carrier distribution (a) and the complex dielectric constant (b) after the excitation by ultrafast laser. E_{pump} indicates the pump photon energy and E_g is the band gap, i.e., the pseudogap in this work. λ_{pump} and λ_g indicate the corresponding wavelengths. In (a), the solid circle represents electrons and the empty circles represents holes. During the cooling, probe with wavelength λ_1 shorter than λ_{pump} always detects $\Delta\varepsilon_1 > 0$ as indicated by the purple dashed line, while probe with wavelength λ_2 between λ_{pump} and λ_g detects $\Delta\varepsilon_1 < 0$ initially and $\Delta\varepsilon_1 > 0$ when the carriers are cooled down to the band edges as indicated by the green dashed line.

the carriers cool down to the band edges by transferring energy to the lattice, band filling shifts to states near the band gap, as illustrated in Fig. 2(a). The ε_2 sink also shifts to the energy of the band gap E_g (the lower red curve in Fig. 2(b), the band gap is also marked as λ_g in the lower part of Fig. 2(b)). For this state, Eq. (1) predicts $\Delta\varepsilon_1 > 0$ for probe wavelength shorter than λ_g. Therefore, probes with wavelength shorter than λ_{pump} as indicated by the purple dashed line in Fig. 2(b) detect $\Delta\varepsilon_1 > 0$. Probes with wavelength between λ_{pump} and λ_g, as indicated by the green dashed line in Fig. 3(b) detect $\Delta\varepsilon_1 < 0$ immediately after the excitation and $\Delta\varepsilon_1 > 0$ after the carriers are cooled down to the band edges. (These two types of wavelengths are used in our experiments.)

The reflectance change is related to the change of the dielectric constant as

$$\frac{\Delta R}{R} = \frac{1}{R}\left(\Delta\varepsilon_1 \frac{\partial R}{\partial \varepsilon_1} + \Delta\varepsilon_2 \frac{\partial R}{\partial \varepsilon_2}\right), \tag{2a}$$

$$\frac{1}{R}\frac{\partial R}{\partial \varepsilon_1} = \frac{(2\varepsilon_1 - |\varepsilon| - 1)\sqrt{2(\varepsilon_1 + |\varepsilon|)}}{|\varepsilon|\left[(\varepsilon_1 - 1)^2 + {\varepsilon_2}^2\right]}, \tag{2b}$$

$$\frac{1}{R}\frac{\partial R}{\partial \varepsilon_2} = \frac{\sqrt{2}\varepsilon_2(2\varepsilon_1 + |\varepsilon| - 1)}{|\varepsilon|\sqrt{|\varepsilon| + \varepsilon_1}\left[(\varepsilon_1 - 1)^2 + {\varepsilon_2}^2\right]}. \tag{2c}$$

Values of the dielectric constant are obtained from the optical conductivity and the reflectance spectrum. For example, the real part of the optical conductivity at 900 nm is $\sigma_1 = 6.4 \times 10^5\ \Omega^{-1}\ \mathrm{m}^{-1}$, rendering the imaginary part of the dielectric constant $\varepsilon_2 = \sigma_1/(\varepsilon_0\omega) = 34.5$ and the reflectance is about 0.6,[22] from which the real part of the dielectric constant $\varepsilon_1 = 5.4$ is derived. From Eqs. (2b) and (2c) and the published data of optical conductivity and reflectance spectrum,[22] it is found that within the entire probe wavelength range used in this work, $\partial R/\partial\varepsilon_1 < 0$ and $\partial R/\partial\varepsilon_2 > 0$. Therefore, right after the excitation, for probe wavelengths longer than $\lambda_{pump} = 800$ nm (e.g., λ_2 in Fig. 2(b)), $\Delta R > 0$ since $\Delta\varepsilon_1 < 0$; while for probe wavelengths shorter than 800 nm (e.g., λ_1 in Fig. 2(b)), $\Delta R < 0$. ($\Delta\varepsilon_2 < 0$ occurs only within a narrow spectrum so that only $\Delta\varepsilon_1$ is considered for the analysis of ΔR). This explains the initial change of reflectance, i.e., increase vs. decrease within the first 1 ps, as shown in Fig. 1. The flip of the sign of reflectivity should occur around the pump wavelength of 800 nm, while Fig. 1 shows this flip occurs at about 1000 nm. The optical reflectance behavior observed in the skutterudite samples presented here is comparable to that observed in GaAs,[31] and can be understood as cooling of the carriers towards the band edges so that band filling occurs at lower photon energy or longer wavelength than that of the pump wavelength.

The effect of free carrier absorption on the reflectance can be evaluated through the dielectric function of a free electron gas[32] and its contribution can be modeled as[29]

$$\frac{\Delta R}{R} = A_{FCA}\frac{erf\left(t/t_p\right) + 1}{2\left[1 + \frac{\Delta m^*}{m^*}\exp\left(-\frac{t}{\tau_{cp}}\right)\right]}. \tag{3}$$

t_p is equal to 0.72 times the full width at half maximum of the laser pulse and the error function accounts for the finite pulse width. A_{FCA} reflects the amplitude of the contribution from free carrier absorption. $\Delta m^*/m^*$ is the relative change of the carrier effective optical mass[29] when the carrier temperature reaches maximum. τ_{cp} is the characteristic time for the carriers and the phonons to reach thermal equilibrium. This model accounts for the evolution of the dielectric function of a free carrier gas as it is cooled down through carrier-phonon scattering. The temperature evolution is manifested in the change in the effective optical mass. As an illustration, this model is used to fit the transient reflectance signal probed at 1000 nm, for which the contribution from band filling is negligible. Figure 3 shows the fitting result together with the fitting parameters. t_p is found to be 80 fs implying a pulse width of 111 fs, which is reasonable considering the dispersion.

For the signals probed by other wavelengths, the contribution from band filling is modeled as follows:[33]

$$\frac{\Delta R}{R} = A_{BF}\frac{erf\left(t/t_p\right) + 1}{2}\exp\left(-\frac{t}{\tau_{cr}}\right), \tag{4}$$

where A_{BF} reflects the amplitude of the contribution from band filling and τ_{cr} is the relaxation time of the carriers at the probed energy level. The sum of Eqs. (3) and (4) is used to fit the entire optical signal. t_p, τ_{cp}, and $\Delta m^*/m^*$ are fixed within the fitting, which should not depend on the energy level. The fitting results for the signals probed by 1500 and 650 nm are shown in Fig. 4 together with the fitting parameters.

From the results displayed in Figs. 3 and 4, we can see that as the probe wavelength decreases across the pump wavelength, the contribution from band filling turns from positive to negative as explained previously. The values of τ_{cr}, which quantify the carrier relaxation time on the probed energy level, are found to be about 0.4–0.6 ps. τ_{cr} is slightly shorter for the probe with shorter wavelength since the dynamics of the carriers in high energy levels are detected.

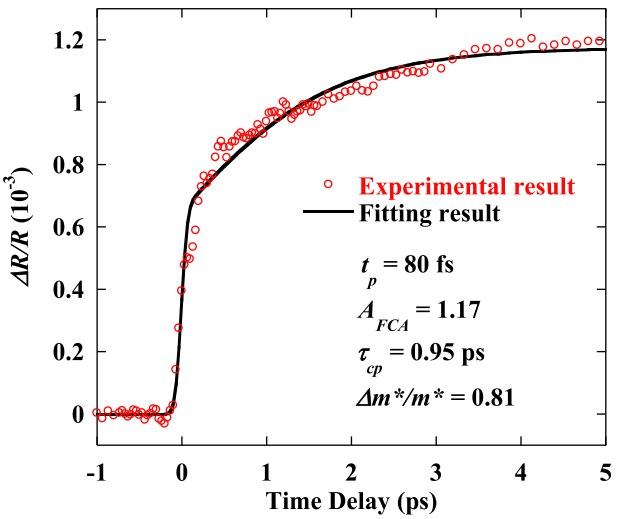

FIG. 3. The transient reflectance signal excited by 0.42 mJ/cm^2 and probed by 1000 nm fit by Eq. (3) modeling the contribution from free carrier absorption.

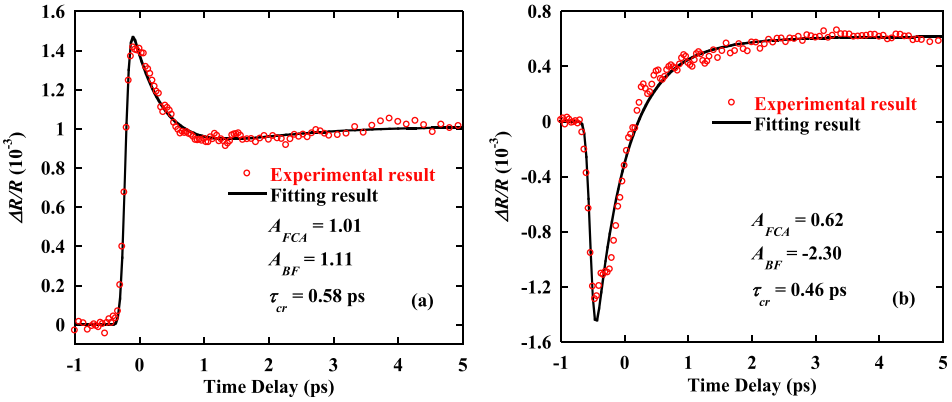

FIG. 4. Transient reflectance signals excited by 0.42 mJ/cm^2 and probed by 1500 (a) and 650 nm (b) fit by Eqs. (3) and (4) modeling the contribution from free carrier absorption and band filling.

These higher energy carriers scatter phonons at a faster rate. From the pump fluence dependence of the signals (not shown), the value of τ_{cr} does not depend on the pump laser fluence or carrier density, which indicates that the relaxation of hot carriers is dominated by carrier-phonon scattering instead of carrier-carrier scattering. The value of τ_{cp}, the characteristic time for the carriers and the phonons to reach the same temperature, is found to be 0.95 ps.

The time constants extracted from the analysis above provides a quantitative evaluation of the carrier dynamics. The carrier relaxation time τ_{cr} detected with different probe wavelengths or energy is proportional to carrier mobility at the corresponding energy level, which is of importance concerning the performance of skutterudites as thermoelectric material. For gaining an understanding of the carrier dynamics at or near equilibrium states, which is the case in most applications, one would be interested in detecting the dynamics of electrons or holes near the band edge. For this case, the photon energy of the pump laser should be lower than the pseudogap energy in order to excite only free carriers, i.e., electrons in *n*-type or holes in *p*-type materials. The photon energy of the probe laser should also be tuned close to the pseudogap so that only band-edge states are probed. Our current experimental capability limits us to the wavelengths range reported above, but the method and the analysis described can be readily extended for such studies.

In summary, ultrafast spectroscopy is applied to study the carrier dynamics in filled-skutterudites. Probing with varied wavelengths shows that the short-time signal after excitation, which is explained by the Kramers-Kronig relation, reflects band filling due to the photoexcited carriers and the signal at longer delay time is due to free carrier absorption. Based on phenomenological models, the analysis shows that the carrier relaxation time is 0.4–0.6 ps for the electronic energy levels detected in this work. The characteristic time for carriers and phonons to reach thermal equilibrium is 0.95 ps. This work illustrates the underlying physical processes during excitation and relaxation of the carriers in different energy levels in skutterudites. Understanding of the carrier dynamics at near-equilibrium states can be achieved by extending the experiments to the mid-IR wavelength range.

The authors would like to acknowledge the support from the National Science Foundation and the Department of Energy under Award No. DE-EE0005432.

[1]G. A. Slack, *CRC Handbook of Thermoelectrics*, edited by D. M. Rowe (CRC, Boca Raton, Florida, 1995).
[2]G. P. Meisner, D. T. Morelli, S. Hu, J. Yang, and C. Uher, Phys. Rev. Lett. **80**, 3551 (1998).
[3]G. S. Nolas, H. Takizawa, T. Endo, H. Sellinschegg, and D. C. Johnson, Appl. Phys. Lett. **77**, 52 (2000).
[4]X. Shi, H. Kong, C.-P. Li, C. Uher, J. Yang, J. R. Salvador, H. Wang, L. Chen, and W. Zhang, Appl. Phys. Lett. **92**, 182101 (2008).
[5]X. Shi, J. Yang, J. R. Salvador, M. F. Chi, J. Y. Cho, H. Wang, S. Q. Bai, J. H. Yang, W. Q. Zhang, and L. D. Chen, J. Am. Chem. Soc. **133**, 7837 (2011).
[6]B. C. Sales, D. Mandrus, and R. K. Williams, Science **272**, 1325 (1996).
[7]T. Caillat, A. Borshchevsky, and J. P. Fleurial, J. Appl. Phys. **80**, 4442 (1996).
[8]G. S. Nolas, D. T. Morelli, and T. M. Tritt, Annu. Rev. Mater. Sci. **29**, 89 (1999).
[9]H. Kleinke, Chem. Mater. **22**, 604 (2010).
[10]W. S. Liu, X. Yan, G. Chen, and Z. F. Ren, Nano Energy **1**, 42 (2012).
[11]L. X. Li, H. Liu, J. Y. Wang, X. B. Hu, S. R. Zhao, H. D. Jiang, Q. J. Huang, H. H. Wang, and Z. F. Li, Chem. Phys. Lett. **347**, 373 (2001).
[12]V. Keppens, D. Mandrus, B. C. Sales, B. C. Chakoumakos, P. Dai, R. Coldea, M. B. Maple, D. A. Gajewski, E. J. Freeman, and S. Bennington, Nature (London) **395**, 876 (1998).
[13]R. P. Hermann, R. Y. Jin, W. Schweika, F. Grandjean, D. Mandrus, B. C. Sales, and G. J. Long, Phys. Rev. Lett. **90**, 135505 (2003).
[14]S. V. Dordevic, N. R. Dilley, E. D. Bauer, D. N. Basov, M. B. Maple, and L. Degiorgi, Phys. Rev. B **60**, 11321 (1999).
[15]M. M. Koza, M. R. Johnson, R. Viennois, H. Mutka, L. Girard, and D. Ravot, Nat. Mater. **7**, 805 (2008).
[16]N. Bernstein, J. L. Feldman, and D. J. Singh, Phys. Rev. B **81**, 134301 (2010).
[17]B. L. Huang and M. Kaviany, Acta Mater. **58**, 4516 (2010).
[18]Y. Wang, X. Xu, and J. Yang, Phys. Rev. Lett. **102**, 175508 (2009).
[19]L. Guo, X. Xu, J. R. Salvador, and G. P. Meisner, Appl. Phys. Lett. **102**, 111905 (2013).
[20]C. He, M. Daniel, M. Grossmann, O. Ristow, D. Brick, M. Schubert, M. Albrecht, and T. Dekorsy, Phys. Rev. B **89**, 174303 (2014).
[21]O. M. Løvvik and Ø. Prytz, Phys. Rev. B **70**, 195119 (2004).
[22]S.-I. Kimura, H. Im, T. Mizuno, S. Narazu, E. Matsuoka, and T. Takabatake, Phys. Rev. B **75**, 245106 (2007).
[23]K. Koga, K. Akai, K. Oshiro, and M. Matsuura, Phys. Rev. B **71**, 155119 (2005).
[24]D. J. Singh and W. E. Pickett, Phys. Rev. B **50**, 11235 (1994).
[25]L. Nordstrom and D. J. Singh, Phys. Rev. B **53**, 1103 (1996).
[26]D. J. Singh and I. I. Mazin, Phys. Rev. B **56**, R1650 (1997).
[27]K. Takegahara, M. Kudoh, and H. Harima, J. Phys. Soc. Jpn. **77**, 294 (2008).
[28]B. R. Bennett, R. A. Soref, and J. A. Del Alamo, IEEE J. Quantum Electron. **26**, 113 (1990).
[29]A. J. Sabbah and D. M. Riffe, Phys. Rev. B **66**, 165217 (2002).
[30]F. Wooten, *Optical Properties of Solids* (Academic Press, New York, 1972).
[31]T. Gong, P. Mertz, W. L. Nighan, Jr., and P. M. Fauchet, Appl. Phys. Lett. **59**, 721 (1991).
[32]C. Kittel, *Introduction to Solid State Physics* (John Wiley & Sons, Inc., Hoboken, New Jersey, 2005).
[33]A. A. Melnikov, O. V. Misochko, and S. V. Chekalin, J. Appl. Phys. **114**, 033502 (2013).